Two-dimensional Fermi plasma in a magnetic field

D. C. Bardos and N. E. Frankel

School of Physics, University of Melbourne, Parkville, Victoria 3052, Australia

(Received 24 June 1993)

We investigate the dielectric response of a planar Fermi plasma in the presence of a constant external magnetic field. The conductivity tensor is derived in the random-phase approximation taking into account the effects of the spin of the electron. This proper inclusion of spin makes a significant difference to the results compared with all previous studies, which ignored the intrinsic spin of the electron. In studying the dispersion relations for the electrodynamic modes of the plasma in an external magnetic field, it is necessary to observe that the longitudinal and transverse modes are coupled. These coupled modes are investigated in some detail.

I. INTRODUCTION

The study of two-dimensional and other lower dimensional many-body systems has developed into a field of its own. These studies have been given new impetus by recent experimental evidence of the role played by planar structures within bulk samples displaying high-T_c superconductivity.[1] One of the earliest two-dimensional quantum many-body systems to receive concerted attention was the two-dimensional electron gas (2DEG).[2] Studies into the 2DEG, which have by now accumulated a vast literature,[3,4] were motivated by the development of semiconductor crystals and associated technology. At sufficiently high applied electric fields, charges accumulating at semiconductor inversion layers were found to behave as if they were restricted to two dimensions, and could be modeled by the 2DEG. This ready access to experimental realizations[3] made the 2DEG an ideal many-body system for theoretical investigation.

The theory of the 2DEG has now become a tool employed by experimentalists for probing semiconductor structure. Random-phase approximation (RPA) plasmon calculations for layered 2DEG structures have been used, for example, to interpret Raman-scattering data and hence determine the electronic structure of modulation-doped GaAs/Al$_x$Ga$_{1-x}$ crystals (see Fasol, Richards, and Ploog[5]). Previous calculations of the dielectric response of the Fermi plasma,[4,6-12] while employing Fermi statistics for the plasma constituents, have not incorporated the electrodynamic effects of spin into their calculations. In this paper a full study of the Fermi plasma conductivity is made without neglecting these effects. We believe that this is the first time spin effects have been included in conductivity calculations for either the plasma layer or the bulk (i.e., three-dimensional) plasma. The proper inclusion of spin will be seen to make significant differences to the results. The formalism should also be applied to the three-dimensional plasma; however, this paper deals solely with the two-dimensional plasma.

In Sec. II the conductivity tensor for the planar Fermi plasma is derived in the self-consistent random-phase approximation, using techniques introduced by Harris.[6] In

Sec. III the tensor is evaluated for a uniform external magnetic field. The zero-temperature conductivity tensor is discussed, and evaluated for high magnetic fields in terms of Kummer hypergeometric functions. In Sec. IV, the results of Sec. III and the dispersion relation for plasma layers, written in terms of conductivity components,[4,13] are combined to yield the dispersion relation for the modes of the planar $T=0$ Fermi plasma. These modes are then investigated in detail for the case of a strong applied magnetic field.

II. CONDUCTIVITY DERIVATION

We now sketch the derivation of the conductivity tensor $\vec{\sigma}$ for the two-dimensional Fermi plasma in the RPA. The formal development is similar to the approach of Harris.[6] It is assumed that the response of the system is such that the perturbations to the external fields are small enough to be treated linearly. We write

$$\mathbf{A} = \mathbf{A}_0 + \mathbf{A}_1, \quad \Phi = \Phi_0 + \Phi_1, \tag{1}$$

where $\mathbf{A}_0$ and Φ_0 are the external potentials, and $\mathbf{A}_1$ and Φ_1 are small perturbations due to the response of the plasma. The second quantized Hamiltonian for a spin $\frac{1}{2}$ charged Fermi field restricted to two dimensions in the presence of an electromagnetic field is written

$$\hat{\mathbf{H}} = \int d^2\mathbf{r}\, \hat{\Psi}^\dagger \mathcal{H} \hat{\Psi}, \tag{2}$$

where the single-particle Hamiltonian $\mathcal{H}$ is that of the Schrödinger-Pauli equation

$$\mathcal{H} = \frac{1}{2\mu}\left[\mathbf{p} - \frac{e}{c}\mathbf{A}\right]^2 + e\Phi - \frac{e\hbar}{2\mu c}\boldsymbol{\sigma}\cdot(\nabla\times\mathbf{A}), \tag{3}$$

where μ is the Fermion mass and $\boldsymbol{\sigma}$ is the Pauli spin operator. The Schrödinger-Pauli current operator is also required:

$$\mathbf{J}(\mathbf{r},t) = \frac{e\hbar}{2\mu i}[\hat{\Psi}^\dagger\nabla\hat{\Psi} - (\nabla\hat{\Psi}^\dagger)\hat{\Psi}] - \frac{e^2}{\mu c}\hat{\Psi}^\dagger\hat{\Psi}\mathbf{A}$$
$$+ \frac{e\hbar}{2\mu}\nabla\times(\hat{\Psi}^\dagger\boldsymbol{\sigma}\hat{\Psi}). \tag{4}$$

In the above, $\hat{\Psi}$ is the second quantized Fermi field operator;

$$\hat{\Psi} = \sum_{p,s} b_{p,s}(t)\psi_{p,s}(\mathbf{r}) , \tag{5}$$

where $b_{p,s}(t)$ is the fermion annihilation operator for the state p,s. The wave functions $\psi_{p,s}(\mathbf{r})$ are the fermion eigenstates of the unperturbed Hamiltonian:

$$\mathcal{H}_0 = \frac{1}{2\mu}\left[\mathbf{p} - \frac{e}{c}\mathbf{A}_0\right]^2 + e\Phi_0 - \frac{e\hbar}{2\mu c}\boldsymbol{\sigma}\cdot(\nabla\times\mathbf{A}_0) . \tag{6}$$

An ensemble-averaging procedure is employed, similar to that previously used in relativistic conductivity[13] and polarization[14] calculations, leading to an expression for the Fourier-transformed current in terms of the electric field $\mathbf{E}$:

$$\mathbf{J}(\mathbf{q},\omega) = \sum_{\mathbf{k}} \overleftrightarrow{\sigma}(\mathbf{q},\mathbf{k},\omega)\cdot\mathbf{E}(\mathbf{k},\omega) , \tag{7}$$

from which the conductivity tensor may be obtained:

$$\overleftrightarrow{\sigma}(\mathbf{q},\mathbf{k},\omega) = \frac{ie^2}{\mu L^2\hbar}\sum_{\substack{p,p'\\s,s'}}\frac{F(\mathbf{p}',s')-F(\mathbf{p},s)}{\omega-(E_{p,s}-E_{p',s'})/\hbar+i\eta}\left\{\langle \mathbf{p}'s'|e^{-i\mathbf{q}\cdot\mathbf{r}}\left[\mathbf{p}-\frac{\hbar}{2}\mathbf{q}-\frac{e}{c}\mathbf{A}_0\right]|s\mathbf{p}\rangle\right.$$

$$+\tfrac{1}{2}(\langle \mathbf{p}'s'|e^{-i\mathbf{q}\cdot\mathbf{r}}\mathbf{p}\times i\boldsymbol{\sigma}|s\mathbf{p}\rangle+\langle \mathbf{p}s|e^{i\mathbf{q}\cdot\mathbf{r}}\mathbf{p}\times i\boldsymbol{\sigma}|s'\mathbf{p}'\rangle^*)\Bigg\}$$

$$\times\left\{\langle \mathbf{p}s|e^{i\mathbf{k}\cdot\mathbf{r}}|s'\mathbf{p}'\rangle\frac{\mathbf{k}}{k^2}+\frac{\hbar}{2\mu\omega}\langle \mathbf{p}s|e^{i\mathbf{k}\cdot\mathbf{r}}i\boldsymbol{\sigma}\times\mathbf{k}|s'\mathbf{p}'\rangle+\frac{1}{\mu\omega}\langle \mathbf{p}s|e^{i\mathbf{k}\cdot\mathbf{r}}\left[\mathbf{p}-\frac{e}{c}\mathbf{A}_0\right]|s'\mathbf{p}'\rangle\cdot\left[\overleftrightarrow{I}-\frac{\mathbf{kk}}{k^2}\right]\right\}$$

$$+\frac{ie^2}{\mu L^2\omega}\sum_{p,s}F(\mathbf{p},s)\langle \mathbf{p}s|e^{i(\mathbf{k}-\mathbf{q})\cdot\mathbf{r}}|s\mathbf{p}\rangle\left[\overleftrightarrow{I}-\frac{\mathbf{kk}}{k^2}\right] , \tag{8}$$

In the above, $F(\mathbf{p},s)$ denotes the equilibrium distribution function for the noninteracting Fermi gas. The usual two-dimensional matrix elements are employed:

$$\langle \mathbf{p},s|\hat{O}|\mathbf{p}',s'\rangle = \int d^2r\,\psi_{p,s}^{\dagger}\hat{O}\psi_{p',s'} . \tag{9}$$

The tensor (8) is valid for all temperatures and applied electromagnetic fields, the effects of which enter through the distribution functions and matrix elements, respectively. The conductivity tensor for the three-dimensional plasma can be obtained from the above result with the substitution of L^3 for L^2, and appropriate interpretation of the matrix elements. The conductivity tensor (8) differs from previous results[4,6-12] due to the correct incorporation of spin terms in the current (4) and Hamiltonian (3) operators.

III. TENSOR EVALUATION

We now evaluate the conductivity tensor (8) for the case of a uniform magnetic field perpendicular to the plane. In order to calculate the matrix elements appearing in this expression, we require the stationary eigenstates of the single-particle Hamiltonian:

$$\psi_{p,s} \equiv \psi_{n,k_x,s} = N_n\phi_n\chi_s ,$$
$$\psi_{p',s'} \equiv \psi_{m,k_x',s'} = N_m\phi_m\chi_{s'} , \tag{10}$$

where χ_s is the Pauli spinor ($s=1, s=-1$ denotes spin up, spin down), and

$$\phi_n = e^{ik_x x - (q_B^2/2)(y+y_0)^2}H_n[q_B(y+y_0)] ,$$

$$N_n = \frac{1}{\sqrt{2^n n! L}}\left[\frac{q_B^2}{\pi}\right]^{1/4} , \tag{11}$$

$$n = 0,1,2\ldots$$

are the usual Landau wave functions and normalizations, with the notation

$$q_B^2 \equiv \frac{\mu\omega_c}{\hbar} ,$$
$$\omega_c \equiv \frac{|e|B}{\mu c} , \tag{12}$$
$$y_0 \equiv \frac{\hbar c k_x}{eB} .$$

Note that the values of $k_x[=(2\pi/L)\times\text{integer}]$ are restricted to the range

$$-\frac{\mu\omega_c L}{2\hbar} < k_x < \frac{\mu\omega_c L}{2\hbar} \tag{13}$$

in order to ensure that the center of gyration lies within the box of length L. The energy is degenerate in k_x, with eigenvalues

$$E_{p,s} = E_{n,s}$$

$$= \left[n + \tfrac{1}{2} - \frac{\text{sgn}(e)}{2} s \right] \hbar \omega_c \ , \tag{14}$$

where $\text{sgn}(e) = \pm 1$ is the sign of the charge. The matrix elements necessary for evaluating the conductivity may be calculated using methods similar to those of found in the Bose case,[15] with some additional complication due to the spin operators. The results are

$$\langle ps | e^{i\mathbf{q}'\cdot\mathbf{r}} | s'p' \rangle = \delta_{k_x', k_x - q_x'} e^{-(\hbar/\mu\omega_c)\{(1/4)(q_x'^2 + q_y'^2) + i\,\text{sgn}(e)[q_y' k_x - (1/2)q_x' q_y']\}}\, {}^nF_m(q')\delta_{s,s'} \ ,$$

$$\langle p's' | e^{-i\mathbf{q}\cdot\mathbf{r}} \left[\mathbf{p} - \frac{\hbar}{2}\mathbf{q} - \frac{e}{c}\mathbf{A} \right] | sp \rangle = \delta_{k_x', k_x - q_x} e^{-(\hbar/\mu\omega_c)\{(1/4)(q_x^2 + q_y^2) - i\,\text{sgn}(e)[q_y k_x - (1/2)q_x q_y]\}}\, \mathbf{M}_1(q)\delta_{s,s'} \ ,$$

$$\langle ps | e^{i\mathbf{q}'\cdot\mathbf{r}} | s'p' \rangle \frac{\mathbf{q}'}{q'^2} + \frac{1}{\mu\omega} \langle p | e^{i\mathbf{q}'\cdot\mathbf{r}} \left[\mathbf{p} - \frac{e}{c}\mathbf{A} \right] | p' \rangle \cdot \left[\vec{I} - \frac{\mathbf{q}'\mathbf{q}'}{q'^2} \right]$$

$$= \delta_{k_x', k_x - q_x} e^{-(\hbar/\mu\omega_c)\{(1/4)(q_x'^2 + q_y'^2) + i\,\text{sgn}(e)[q_y' k_x - (1/2)q_x' q_y']\}}\, \mathbf{M}_2(q')\delta_{s,s'} \ , \tag{15}$$

$$\langle p's' | e^{-i\mathbf{q}\cdot\mathbf{r}} \mathbf{p} \times i\boldsymbol{\sigma} | sp \rangle + \langle ps | e^{i\mathbf{q}\cdot\mathbf{r}} \mathbf{p} \times i\boldsymbol{\sigma} | s'p' \rangle^* = \delta_{k_x', k_x - q_x} e^{-(\hbar/\mu\omega_c)\{(1/4)(q_x^2 + q_y^2) - i\,\text{sgn}(e)[q_y k_x - (1/2)q_x q_y]\}}\, \mathbf{M}_3(q)s\delta_{s,s'} \ ,$$

$$\langle ps | e^{i\mathbf{q}'\cdot\mathbf{r}} i\boldsymbol{\sigma} \times \mathbf{q}' | s'p' \rangle = \delta_{k_x', k_x - q_x} e^{-(\hbar/\mu\omega_c)\{(1/4)(q_x'^2 + q_y'^2) + i\,\text{sgn}(e)[q_y' k_x - (1/2)q_x' q_y']\}}\, \mathbf{M}_4(q')s\delta_{s,s'} \ ,$$

where the functions $\mathbf{M}_1(q)$, $\mathbf{M}_2(q')$ and ${}^nF_m(q)$ have been defined in Eqs. (14) and (15) of the preceding paper,[15] and the following further definitions have been employed:

$$\mathbf{M}_3(q) = \left\{ \begin{array}{c} \left[\dfrac{\hbar\mu\omega_c}{2} \right]^{1/2} [\sqrt{n}\, {}^{n-1}F_m^*(q) + \sqrt{m}\, {}^nF_{m-1}(q) \\ - \sqrt{n+1}\, {}^{n+1}F_m^*(q) - \sqrt{m+1}\, {}^nF_{m+1}^*(q)] \\[2mm] -i\hbar q_x\, {}^nF_m^*(q) \end{array} \right\} \ , \tag{16}$$

$$\mathbf{M}_4(q') = \left\{ \begin{array}{c} -i\, {}^nF_m(q')q_y' \\ i\, {}^nF_m(q')q_x' \end{array} \right\} \ .$$

Using these matrix elements, the conductivity tensor becomes

$$\vec{\sigma}(\mathbf{q},\mathbf{q}';\omega) = \frac{ie^2}{\mu L^2 \hbar} \sum_{\substack{n,m \\ k_x, k_x' \\ s,s'}} \frac{F(m,s') - F(n,s)}{\omega - (E_{n,s} - E_{m,s'})/\hbar + i\eta} \left[\mathbf{M}_1(q) + \frac{s}{2}\mathbf{M}_3(q) \right] \left[\mathbf{M}_2(q') + \frac{s}{2}\frac{\hbar}{\mu\omega}\mathbf{M}_4(q') \right]$$

$$\times e^{-(1/q_B^2)\{(2q_x^2 + q_y^2 + q_y'^2)/4 + i\,\text{sgn}(e)[k_x(q_y' - q_y) + (q_x/2)(q_y - q_y')]\}} \delta_{k_x', k_x - q_x} \delta_{q_x', q_x} \delta_{s,s'}$$

$$+ \frac{ie^2}{\mu L^2 \omega} \sum_{n, k_x, s} F(n,s) L_n \left[\frac{(q_y' - q_y)^2}{2q_B^2} \right] \left[\mathbf{I} - \frac{\mathbf{q}'\mathbf{q}'}{q'^2} \right]$$

$$\times e^{-(1/q_B^2)\{(1/4)(q_y' - q_y)^2 + i\,\text{sgn}(e)(q_y' - q_y)k_x\}} \delta_{q_x', q_x} \ , \tag{17}$$

where we have made explicit the independence of the distribution function $F(\mathbf{p},s)$ from k_x. This independence results from the k_x degeneracy of the eigenstates $\psi_{n,k_x,s}$ due to the spatial uniformity of the magnetic field. The sums over k_x' and s' collapse, while the k_x sum yields

$$\sum_{k_x} e^{-i(\text{sgn}(e)/q_B^2)(q_y' - q_y)k_x} \rightarrow \frac{L}{2\pi} \int_{-\mu\omega_c L/2\hbar}^{\mu\omega_c L/2\hbar} dx\, e^{-i(\text{sgn}(e)/q_B^2)(q_y' - q_y)k_x} = g\delta_{q_y', q_y} \ , \tag{18}$$

where g denotes Landau degeneracy

$$g = \frac{\mu\omega_c L^2}{2\pi\hbar} \ , \tag{19}$$

and the restriction on the allowed range of values for k_x has been used. Thus the tensor may be written in the form (consistent with the plasma's rotational symmetry)

$$\vec{\sigma}(\mathbf{q},\mathbf{q}',\omega) = \vec{\sigma}(\mathbf{q},\omega)\delta_{\mathbf{q},\mathbf{q}'} \ ,$$

$$\vec{\sigma}(\mathbf{q},\omega) = \frac{ie^2\omega_c}{2\pi\hbar^2}e^{-(q^2/2q_B^2)}\sum_{\substack{n,m \\ s}}\frac{F(m,s)-F(n,s)}{\omega-(E_{n,s}-E_{m,s})/\hbar+i\eta}$$

$$\times\left[\mathbf{M}_1(q)+\frac{s}{2}\mathbf{M}_3(q)\right]\left[\mathbf{M}_2(q)+\frac{s}{2}\frac{\hbar}{\mu\omega}\mathbf{M}_4(q)\right]+\frac{ie^2\rho}{\mu\omega}\left[\mathbf{I}-\frac{\mathbf{qq}}{q^2}\right] \ , \quad (20)$$

where the number density $\rho=(N/L^2)$ has been introduced. This expression for the conductivity tensor is valid for all magnetic-field strengths and temperatures, and differs substantially from tensors derived by previous authors. In particular, many terms in this expression (all those proportional to s) are due to the inclusion of spin operators in the current and Hamiltonian operators used to derive the tensor. These terms were neglected by previous authors either through the use of incomplete operators in RPA treatments (e.g., Harris[6] and Chiu and Quinn[4]) or through expressly longitudinal treatments using the Green's-function approach (e.g., Horing and Yildiz,[8] and Glasser[12]).

Zero-temperature conductivity components

We now investigate the components of the tensor at zero temperature, with particular attention to the spin terms. We take $q_x=0$ for consistency with previous papers[4,13] and for expediency when the components are applied to the dispersion relation in Sec. IV. For the remainder of the paper, we take $\mathrm{sgn}(e)=1$.

In contrast to the three-dimensional case, there is no continuum of energy levels for each Landau level. As a consequence, the Fermi energy E_f is defined by the inequality

$$E_{n_f,1} \leq E_f < E_{n_f,-1} \ , \quad (21)$$

where n_f is the highest occupied Landau level. The $T=0$ distribution function is

$$F(n,s)=\begin{cases} 1, & (n,s)\in\{(n\leq n_f-1,1),(n<n_f-1,-1)\} \\ g', & (n,s)\in\{(n_f-1,-1),(n_f,1)\} \\ 0, & (n,s)\in\{(n>n_f,1),(n\geq n_f,-1)\} \ , \end{cases}$$

$$(22)$$

which reflects the energy degeneracy of opposing spin-states in adjacent Landau levels (i.e., $E_{n,1}=E_{n-1,-1}$). The factor g' is the occupation fraction for the highest occupied energy levels. These levels possess a full complement of degenerate states, but obviously not all such states can be filled except at particular magnetic-field strengths where the number of fermions is an odd multiple of the Landau degeneracy g. If the total number of fermions is N, then the requirement

$$N=\sum_{n,k_x,s}F(n,s)$$

$$=g\sum_{n,s}F(n,s) \quad (23)$$

yields the occupation fraction

$$g'=\begin{cases} \dfrac{N-g(2n_f-1)}{2g}, & n_f\neq0 \\ \dfrac{N}{g}, & n_f=0 \ , \end{cases} \quad (24)$$

with the restriction

$$0<g'\leq1 \quad (25)$$

to ensure consistency with the definition of n_f.

We now investigate expression (20) for the conductivity tensor, using the zero-temperature distribution function (22). We first consider terms proportional either to $\mathbf{M}_1(q)(s/2)(\hbar/\mu\omega)\mathbf{M}_4(q)$ or $(s/2)\mathbf{M}_3(q)\mathbf{M}_2(q)$. Only the two highest Landau levels n_f and n_f-1 can contribute to these terms. For each lower level, the opposing spin states cancel each other due to the appearance of the spin label s in these terms. The contribution of the upper levels depends on g', which oscillates as a function of the magnetic-field strength B. If the field is such that $g'=1$, the opposing spin states in level n_f-1 cancel completely, so the only contribution is from the $(n_f,1)$ states. If the B field then increases, the occupation fraction g' will decrease, leading to incomplete cancellation in the n_f-1 level, and decreasing contribution from the $(n_f,1)$ states. Further increase of the field strength results in g' returning to 1, while n_f decreases by 1. So without evaluating these terms in detail, it is clear that their sum will oscillate as a function of the field as the dominant contribution shifts back and forth between the n_f and n_f-1 Landau levels.

For small magnetic fields, the number of filled levels is large, and the degeneracy factor small. Consequently the "ripples on the Fermi sea" described above are of negligible magnitude, and indeed these contributions vanish entirely as $B\rightarrow0$. Thus, in the small field case, the only contribution to the tensor from the spin terms must be from the $\frac{1}{4}(\hbar/\mu\omega)\mathbf{M}_3(q)\mathbf{M}_4(q)$ term. Inspecting the definitions of $\mathbf{M}_3$ and $\mathbf{M}_4$ it is clear that when $q_x=0$, only the σ_{xx} component of the tensor contains contributions from the spin terms as $B\rightarrow0$. This observation is consistent with the zero-field results for the conductivity

components.[13]

For large field strengths, where the number of Landau levels is small and the degeneracy factor large, the "ripples" become larger in magnitude, until a critical field strength B_c is reached, above which only the spin-up states are occupied (i.e., all fermions are in the lowest Landau level, with spin-up). At the critical field strength, the Landau degeneracy g must equal the number of fermions, yielding the value

$$B_c = \frac{2\pi\hbar c\rho}{|e|} \ . \tag{26}$$

This can be expressed in terms of our scaled parameters as

$$\chi_c = \frac{1}{2\alpha_e}\bar{\rho} \ , \tag{27}$$

where α_e is the fine-structure constant. We now evaluate the tensor in the region $B > B_c$, which has the advantage of simplifying the calculations, while also highlighting the electrodynamic spin effects which we are interested in. In this high-B field region, the statistical differences between the Fermi and Bose plasmas have in effect been suppressed. Thus in order to assess the effect of the spin terms in the $B > B_c$ region, we need only compare the results for the Fermi plasma with the corresponding results for the Bose plasma.[15]

Considering the expression (20) for the conductivity tensor, we immediately take the limit $\eta \to 0$, with the condition that $\omega \neq m\omega_c$, where m is an integer. Applying the definitions (16) of $\mathbf{M}_3$ and $\mathbf{M}_4$ (see preceding paper[15] for $\mathbf{M}_1, \mathbf{M}_2$), the zero-temperature temperature distribution function (22) and the Kummer function formulas,[15] we can write the components of the conductivity tensor for $B > B_c$ in terms of the Kummer functions:

$$\sigma_{yy}^{B>B_c}(q,\omega_r) = \frac{i\rho e^2}{2\mu\omega_c} \frac{\Phi(1,1-x,-z)-\Phi(1,1+x,-z)}{z} \ ,$$

$$\sigma_{xx}^{B>B_c}(q,\omega_r) = \frac{i\rho e^2}{2\mu\omega_c} \frac{\Phi(1,1-x,-z)-\Phi(1,1+x,-z)}{z} \ ,$$

$$\sigma_{yx}^{B>B_c}(q,\omega_r) \tag{28}$$

$$= \frac{\rho e^2}{2\mu\omega_c} \left\{ \frac{\Phi(1,1-x,-z)+\Phi(1,1+x,-z)}{z} - \frac{2}{z} \right\}$$

$$= -\sigma_{xy}^{B>B_c}(q,\omega_r) \ ,$$

where we have used the notation $x = \omega/\omega_c$ and $z = q^2/2q_B^2$ for the scaled frequency and wave number squared. Comparing these results with the corresponding Bose results,[15] we note that the "longitudinal" component σ_{yy} is unaffected by the spin terms, while σ_{xx}, σ_{yy}, and σ_{yx} are significantly simpler than the corresponding Bose components. We also note that for $B > B_c$, $\sigma_{yy}(q,\omega_r) = \sigma_{xx}(q,\omega_r)$, which is not the case for the Bose plasma. Examination of the structure of the Bose and Fermi conductivity tensors reveals that the difference between them, due to spin, is of order $z (= \hbar q^2/2\mu\omega_c)$, which is the natural wave-number parameter of the magnetized plasma. Thus any physical properties of the system which depend on σ_{xx} or σ_{yx} at wave numbers where first- or higher-order terms in z are required will be materially affected by the correct inclusion of spin.

IV. DISPERSION RELATIONS

We now use the results of previous sections to investigate the modes of electrodynamic oscillation for the planar magnetized Fermi plasma, with particular attention to the zero-temperature $B > B_c$ case. Plasma oscillations must satisfy the dispersion relation[4,13]

$$\left[i\sigma_{xx}(q,\omega) - \frac{\beta c^2}{2\pi\omega} \right] \left[i\sigma_{yy}(q,\omega) + \frac{\omega}{2\pi\beta} \right]$$

$$+ \sigma_{xy}(q,\omega)\sigma_{yx}(q,\omega) = 0 \ . \tag{29}$$

where the conductivity tensor and the plasmon frequency $\omega(q)$ may in general have both real and imaginary parts. In order to decouple the dispersion relation into separate equations for the real and imaginary parts of the plasmon frequency, it is useful to employ the small damping approximation.[6] The imaginary part of the solution $\omega(q)$ to the dispersion relation is called the damping constant, denoted by γ. If we assume that γ, $\mathrm{Re}[\sigma_{xx}]$, $\mathrm{Re}[\sigma_{yy}]$, $\mathrm{Im}[\sigma_{xy}]$, and $\mathrm{Im}[\sigma_{yx}]$ are small, then the real part ω_r of the plasmon frequency is the solution of

$$\left[-\mathrm{Im}[\sigma_{xx}(q,\omega_r)] - \frac{\beta_r c^2}{2\pi\omega_r} \right] \left[-\mathrm{Im}[\sigma_{yy}(q,\omega_r)] + \frac{\omega_r}{2\pi\beta_r} \right] + \mathrm{Re}[\sigma_{xy}(q,\omega_r)]\mathrm{Re}[\sigma_{yx}(q,\omega_r)] = 0 \ . \tag{30}$$

From the form of the conductivity tensor (20) it is clear that $\mathrm{Re}[\sigma_{yy}] = \mathrm{Re}[\sigma_{xx}] = \mathrm{Im}[\sigma_{xy}] = \mathrm{Im}[\sigma_{yx}] = 0$ for any temperature and magnetic field, provided $x \neq$ integer. Consequently the weak damping approximation is appropriate, and indeed it can be shown that the plasmons are undamped (i.e., $\gamma = 0$). In view of the complexity of the conductivity tensor, it is clear that even at zero temperature, extensive numerical work is required in order to investigate the dispersion relation over the full range of magnetic-field strengths, densities, and wave numbers. By way of an initial investigation, we choose to concentrate on the $B > B_c$ case, which is particularly useful because it is analytically tractable and affords an interesting comparison with the dispersion relation of the magnetized Bose plasma.

Zero-temperature, $B > B_c$ dispersion relation

Substituting the zero-temperature conductivity components for $B > B_c$ and $x \neq$ integer displayed in Eq. (28) into the dispersion relation (30) yields the following:

$$\left[\frac{\Phi(1,1+x,-z) - \Phi(1,1-x,-z)}{z} - \frac{\sqrt{z-\chi x^2}}{\lambda x} \right] \left[\frac{\Phi(1,1+x,-z) - \Phi(1,1-x,-z)}{z} + \frac{\chi}{\lambda} \frac{x}{\sqrt{z-\chi x^2}} \right]$$

$$- \left[\frac{\Phi(1,1-x,-z) + \Phi(1,1+x,-z)}{z} - \frac{2}{z} \right]^2 = 0, \quad x \neq n, \quad (31)$$

where the scaled density $\lambda = \pi \rho e^2 q_B^{-1}/\sqrt{2}\mu c^2$ and scaled field strength $\chi = \hbar \omega_c/2\mu c^2$ have been introduced.

This dispersion relation is formally less cumbersome than the corresponding Bose dispersion relation[15] as a result of the simpler expressions for the conductivity components in the Fermi case.

As discussed previously,[15] the form of the two-dimensional plasmon dispersion relation is such that for laboratory scale magnetic fields, the degree of longitudinal-transverse coupling is controlled by the proximity of the dispersion relation to the light cone. Adopting the notation

$$t_{yy} = -\text{Im}[\sigma_{yy}] \frac{2\mu\omega_c}{\bar{\rho}e^2},$$

$$t_{xx} = -\text{Im}[\sigma_{xx}] \frac{2\mu\omega_c}{\bar{\rho}e^2}, \quad (32)$$

$$t_{yx} = \text{Re}[\sigma_{yx}] \frac{2\mu\omega_c}{\bar{\rho}e^2},$$

we now investigate solutions of the "transverse branch"

$$t_{xx} - \frac{\sqrt{z-\chi x^2}}{\lambda x} = 0 \quad (33)$$

near the light cone for the Fermi plasma. Neglecting all but the first term in the Landau series for t_{xx} yields

$$t_{xx} \sim 2xe^{-z} \frac{1}{1-x^2}, \quad (34)$$

which is somewhat different from the corresponding Bose result.[15] Nevertheless, if we consider the nth Bernstein mode (i.e., $x \sim n$) and note that $x \sim q/2\chi$ in the vicinity of the light cone, then $\bar{q} \sim 2n\chi$. Now $\chi \ll 1$ for laboratory scale field strengths, and consequently, if n is not extremely large, $z \ll 1$. Thus terms of order z in t_{xx} can be neglected, yielding

$$t_{xx} \sim \frac{2x}{1-x^2}, \quad (35)$$

which is identical to the Bose result to this order, and leads to the same dispersion relation.[15] We find numerically that this dispersion relation is a very good approximation to the exact equation (31) in the region below $x = 1$, except in the immediate vicinity of the resonance. Thus the magnetized plasma supports essentially transverse oscillations (with a small longitudinal component) for frequencies slightly less than ω_c and below. A typical example of a plasmon dispersion curve in this region (cal-

culated using the full dispersion relation) is shown in Fig. 1. This coincides, in the region shown, almost exactly with the solution of the transverse branch, which can be expressed as a cubic[15] in x^2 if terms of order z or higher are neglected. The numerical results for the Fermi plasmon spectrum displayed in Fig. 1 are different than the corresponding Bose results due to the spin effects. However, the differences, which are of order z, are too small to be resolved graphically because z is extremely small in the transverse region.

Approximately transverse oscillations can also occur at frequencies above $x = 1$ if x is close enough to one of the higher resonances. For $x \sim n$ only the resonance term and the first term in the Landau sum for t_{xx} need be retained

$$t_{xx} = 2xe^{-z} \left[\frac{1}{1-x^2} + \frac{z^{n-1}}{(n-1)!(n^2-x^2)} \right]. \quad (36)$$

This has a simpler structure than the corresponding Bose result;[15] however, they are the same to leading order in small quantities (z and $n^2 - x^2$). Thus, as in the Bose case, the $n > 1$ Bernstein modes terminate at the light cone slightly below $x = n$. The cutoff frequency for each mode, denoted x_n^{min}, is given[15] by

$$x_n^{\text{min}} = n \left[1 - \frac{(n^2-1)(\chi n^2)^{n-1}}{n^2(n-1)!} \right]^{1/2}, \quad (37)$$

which applies for both the Bose and Fermi quantum plasmas (neglecting extremely small differences due to the
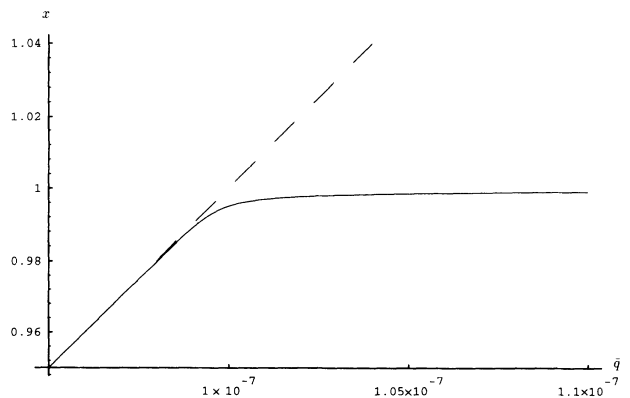

FIG. 1. Large-B dispersion relation (smooth curve) in the transverse region, shown with the light cone $x = \bar{q}/2\chi$ (dashed line). Parameter values are $\chi = 5 \times 10^{-8}$, $\bar{\rho} = 10^{-10}$.

differences in σ_{xx}). The frequency range of each Bernstein mode below $x = n$, i.e., $n - x_n^{min}$, differs in the quantum case discussed here from the result of Chiu and Quinn[4] for the semiclassical plasma. This is due to different structure of the small wave-number expansions of the semiclassical and quantum conductivity tensors. The modes are essentially transverse very near the cutoff, but rapidly deviate from the light cone and become strongly coupled, cross over the resonance, and become more longitudinal with increasing wave number.

We have shown previously[13] that the unmagnetized two-dimensional Fermi plasma does not support transverse plasmons. As an aside, we note that Gudmundsson, Toyoda, and Takahashi[16] have discussed transverse plasmons in zero-β plasma layers. However, their dispersion relation was derived in the limit of large layer thickness and is therefore relevant to anisotropic bulk plasmas rather than two-dimensional plasmas. In the zero thickness limit under consideration here, no transverse plasmons were found.[16]

Thus the existence of transverse modes in the magnetized plasma is an interesting result. For $x < 1$ the transverse solution is "pinned" very tightly to the light cone, and remains so for a much larger range of frequencies than the longitudinal mode near the light cone in the unmagnetized plasma. Physically, the tendency of the unrestricted (i.e., three-dimensional) plasma to support plasma oscillations at approximately the Larmor frequency at large field strengths is in conflict with the retardation effect due to the clamping of the two-dimensional plasma in the z direction. This results in the "clinging" of the dispersion curve more tightly to the light cone with increasing field strength.

The deviation of the plasmon curve in Fig. 1 from the light cone near $x = 1$ signals the onset of a rapid increase in the longitudinal component of the plasma oscillation, which is negligible in Fig. 1 but becomes significant closer to $x = 1$. The strongly coupled region is shown in Fig. 2, where a numerical solution of the full coupled dispersion
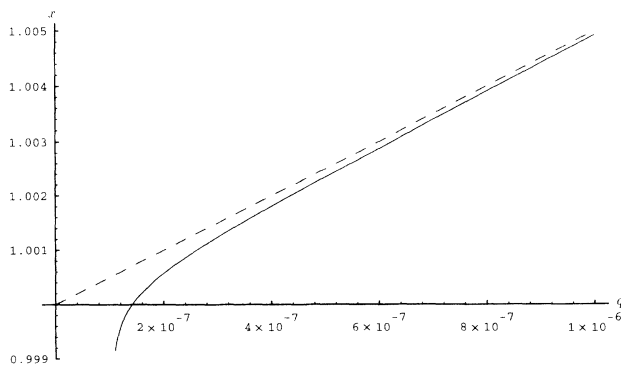
relation is displayed. The dispersion curve crosses over the resonance and becomes increasingly longitudinal with larger wave numbers. We have plotted the coupled dispersion relation against the small wave-number nonretarded solution $x^2 = 1 + (\bar{p}\,\bar{q}/4\chi^2)$ of the longitudinal branch. This was originally derived by Horing and Yildiz,[8] and is identical to the $n = 1$ Bose result[15] because σ_{yy} is identical for the Bose and Fermi plasmas when $B > B_c$.

We note that in their study of dispersion in the semiclassical electron plasma, Chiu and Quinn[4] derived a quadratic equation in the retardation factor β by neglecting all but the first term in the Landau summations in the coupled dispersion relation. This leads to an explicit solution for β as a function of ω, which can then be rearranged as a solution for the wave number q as a function of ω. This solution is also appropriate for the quantum plasmas since the approximation involves only the leading term in the small wave-number expansion of the conductivity tensors. For $x < 1$ this solution approaches the transverse solution discussed earlier, while for $x > 1$ the solution becomes approximately longitudinal. Chiu and Quinn did not, however, discuss the physical nature of this solution in the various regions. Their graph (Fig. 1, Chiu and Quinn[4]) of the solution incorrectly indicates that the dispersion relation lies close to the light cone in the region $1 < x < 2$. In fact the solution is far below the light cone in that region.

We now investigate the dispersion relation for wave numbers large enough that the plasmons are almost completely longitudinal. In Fig. 3 we display the lowest three Bernstein mode solutions to the full dispersion relation (31) for $\chi = 10^{-8}$ and $\bar{p} = 10^{-10}$. For an electron plasma these parameters correspond to a magnetic-field strength of 8.8×10^5 G and an electron number density of 1.5×10^{12} cm^{-2}. The critical field strength [see Eq. (26)] at this density is 6.0×10^5 G.

It is clear from Fig. 3 that the plasmon dispersion curve for the magnetized plasma is composed of an infinite number of distinct modes, each of which occupies a frequency domain of size ω_c. In the case of the lowest (or fundamental) mode, the dispersion curve extends for a further ω_c down to zero frequency; however, it has al-

FIG. 2. Large-B dispersion (smooth line) in the strong-coupling region, compared with the nonretarded longitudinal approximation: $x^2 = 1 + (\bar{p}\bar{q}/4\chi^2)$ (dashed line). As in Fig. 1, the parameters are: $\chi = 5 \times 10^{-8}$, $\bar{p} = 10^{-10}$.
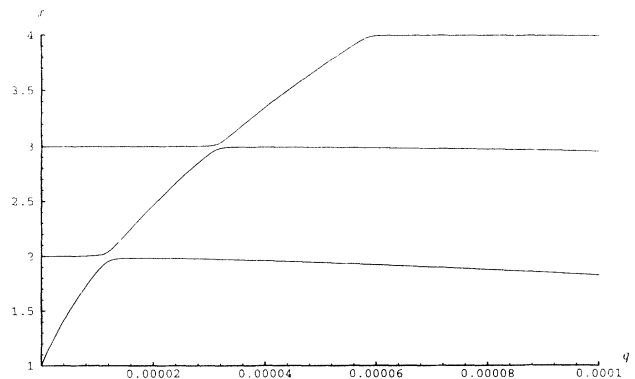

FIG. 3. Solutions of the full dispersion relation (31) in the region where the plasmons are approximately longitudinal. The field strength and density parameters are $\chi = 10^{-8}$, $\bar{p} = 10^{-10}$.

ready been shown that the $0 < x < 1$ region is essentially a transverse mode. In this field strength regime it is meaningful to speak of a "principal plasmon mode," valid for all frequencies not too close to integers $n > 1$; however, this "principal mode" actually consists of segments from each of the Bernstein modes. Although many terms in the Landau series appearing in the conductivity tensor must be retained to describe the higher Bernstein modes near the resonances, the first term provides a useful approximation of the spectrum even in the higher frequency region, provided x is not close to an integer.

In Fig. 4 the three lowest Bernstein modes are plotted for the same density, but the field strength has been increased by a factor of 5. The qualitative structure of the modes has changed drastically. Large gaps in the plasmon frequency spectrum have appeared. The Bernstein mode associated with each resonance lies close to the resonance at small $\bar{q}$, and rises to a maximum frequency as q increases before slowly falling back to the resonance with increasing wave number. No plasmons can propagate at frequencies between the maximum and the next-highest resonance. At this field strength the notion of a "principal mode" is no longer applicable because the discrete character of the Bernstein modes has been asserted, destroying the simple connection between the dispersion in different cyclotron frequency domains which exists at lower field strengths. The results of Fig. 4 are directly comparable with those for the Bose plasma (see the modes in Fig. 3 in the preceding paper,[15] which were calculated for the same field strength). We find that the difference between the Bose and Fermi results is numerically very small, despite the significant differences in the respective conductivity tensors due to spin effects in the Fermi plasma. This is because the dispersion relation at the wave numbers displayed is dominated by the longitudinal branch, which is identical for both cases.

Finally, in Fig. 5 the field strength has been increased further still. Plasmons can propagate only at frequencies in narrow bands above the cyclotron resonances. The applied magnetic field now totally dominates the physics of collective modes in the plasma.
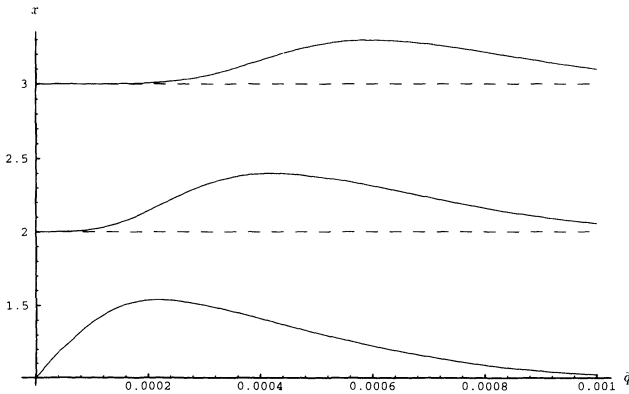

FIG. 4. Solutions of the full dispersion relation (31) in the approximately longitudinal region reveal large gaps in the plasmon frequency spectrum at high field strengths. The field strength here is $\chi = 5 \times 10^{-8}$, a fivefold increase on Fig. 3. The density remains the same: $\bar{p} = 10^{-10}$.
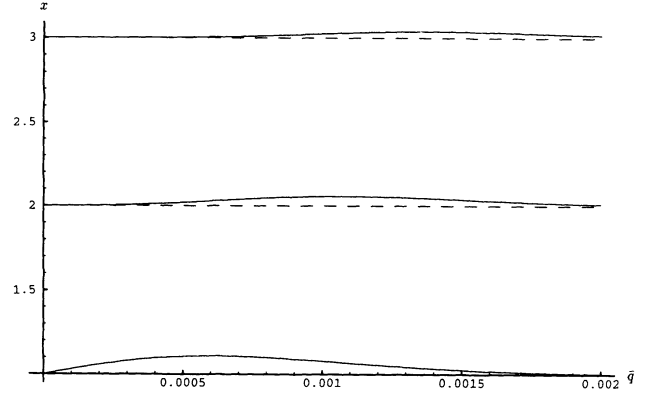

FIG. 5. Here the field strength has been increased from that in Fig. 4 by a further factor of 4 ($\chi = 2 \times 10^{-7}$), resulting in correspondingly larger gaps in the plasmon spectrum. The density remains at $\bar{p} = 10^{-10}$.

V. DISCUSSION

In a previous study of the magnetized plasma layer, Horing and Yildiz[8] examined plasmon dispersion and static screening properties. The plasmons were assumed to be purely longitudinal (i.e., the coupling was neglected) and retardation effects were ignored. In our study of the quantum plasma layers, we have investigated wavenumber regions in which retardation and coupling cannot be neglected (where the plasmons contain a strong transverse component), and also the shorter wavelength regimes where the longitudinal nonretarded treatment approximates the complete treatment to high accuracy. Before comparing our results with those of Horing and Yildiz[8] for the latter "longitudinal region," the validity of neglecting retardation and coupling in the context of realizable plasma layers is examined.

We consider an electron layer of density $\bar{p} = 10^{-10}$, i.e., $\rho = 1.5 \times 10^{12}$ cm^{-2}. In the absence of an applied magnetic field, the wave-number region where retardation is important is scaled by the density. In this case the dispersion relation, obtained by Stern,[2] crosses over from the light cone $\bar{\omega} = \bar{q}$ to $\bar{\omega} = \sqrt{\bar{p}\bar{q}}$ at approximately $\bar{q} = \bar{p}$. In the present example, this means $\bar{q} = 10^{-10}$, or a physical wave number of $q \sim 2.6$ cm^{-1}. Thus the plasmon wavelength is in the centimeter range. By contrast, plasmon experiments are carried out[5] at wave numbers of order 10^5 cm^{-1}, where retardation is obviously negligible. In the case of a strong applied magnetic field, however, the retardation region is scaled by the cyclotron frequency. The crossover from the light cone into the strongly coupled region occurs around $x = 1$, i.e., $q \sim \omega_c / c$, or in scaled variables $\bar{q} \sim 2\chi$. We now make use of numerical results for a field strength of 4.4×10^7 G (i.e., $\chi = 5 \times 10^{-7}$). The results displayed for the Bose plasma[15] are indistinguishable graphically from equivalent Fermi results in the strong-coupling region, which are not displayed for this particular field strength. This similarity occurs because the parameter z is very small at the relevant wavelengths (i.e., in the strong-coupling region),

with the result that corrections due to spin are extremely small in this region. The plasmon mode crosses below the cyclotron frequency (signaling the dominance of the transverse branch) for $\bar{q} < 1.4 \times 10^{-6}$, corresponding to wave numbers $q < 0.36 \times 10^5$ cm^{-1}, which are in the range accessible to experiments, subject to the availability of sufficiently strong fields. At slightly larger wave numbers (e.g., $\bar{q} = 2 \times 10^{-6}$, i.e., $q = 0.52 \times 10^5$ cm^{-1}), the plasmon frequency ω is greater than ω_c, but the difference $\omega - \omega_c$ is roughly half that obtained by neglecting coupling and retardation, indicating that in this region the plasmons have substantial transverse components.

An interesting feature of the coupled dispersion relation (29) is the role played by retardation effects in controlling the importance of the transverse branch. As the plasmon dispersion curve approaches the light cone the plasmons become increasingly transverse, in contrast to the unmagnetized plasma, where no transverse plasmons occur either in the retardation region or at higher wave numbers. In many previous studies[8,11,12] of the magnetized plasma layer, retardation and coupling have been neglected, despite the early work of Chiu and Quinn[4] in which the full coupled dispersion relation, written in terms of the conductivity tensor, was presented.

At larger wave numbers or weaker field strengths than those discussed above, the plasmons become increasingly longitudinal. By expanding the longitudinal polarizability (i.e., χ_{yy}) for small values of the parameter $z = \hbar q^2 / 2\mu\omega_c$ (i.e., a small wave-number expansion valid for intermediate or high fields), Horing and Yildiz derived the following dispersion relation:

$$\omega^2 = \omega_c^2 + \frac{2\pi e^2 \rho q}{\mu} . \tag{38}$$

In the above equation ρ is a simple number density only when $B > B_c$. When $B < B_c$, ρ exhibits de Haas–van Alphen oscillations. In our scaled notation the dispersion relation (38) can be written as $x^2 = 1 + (\bar{\rho}\bar{q}/4\chi^2)$ for $B > B_c$. This formula approximately describes the dispersion curves in Fig. 3 except near the resonances at integer values of x. Thus Eq. (38) can be regarded as an approximation to the "principal mode" which is in fact constructed from segments of the various Bernstein modes.

The discussion[8] refers to a crossover of the principal mode and the $n = 2$ Bernstein mode at $x = 2$, where they "strongly interact." This is meaningless in the sense that the principal mode is composed of the Bernstein modes and cannot interact with them. The fundamental plasmon mode (i.e., the $n = 1$ Bernstein mode) cannot cross over $x = 2$.

At higher field strength (see Figs. 4 and 5), formula (38) no longer provides a useful approximate description of the modes in the higher frequency regions, because the "principal mode" has broken up due to the stronger influence of the cyclotron resonances. The fundamental mode turns away drastically from (38) well below the resonance at $x = 2$. Higher-order terms in the expansion are required to reproduce this behavior. Similarly, many terms in the Landau summations appearing in the disper-

sion relation must be retained to adequately describe the higher Bernstein modes.

In the $B \to 0$ limit, the dispersion relation (38) yields the correct zero-B Stern result[2] for the nonretarded region, as noted in Horing and Yildiz.[11] However, we argue below that the small-B corrections to the plasmon frequency given by the formula (38), which are of order B^2, are incorrect. Although we have not presented a $B \to 0$ analysis for the Fermi plasma, we note that in the Bose plasma the leading-order small-B corrections were of order B. We would expect this to carry over to the Fermi case because the leading-order magnetic-field corrections in the Bose case depended only on the longitudinal part of the dispersion relation, and consequently would be unaffected by the spin terms in the Fermi conductivity. The wave-number and density structure of the magnetic-field corrections would be expected to be different due to the large number of Landau levels occupied, as dictated by the Fermi statistics; but we would not expect the linear term present in the Bose expansion to vanish in the Fermi case. In the Fermi case there will of course be de Haas–van Alphen oscillatory terms, but they will be exponentially small as $B \to 0$. The result of Horing and Yildiz cannot be applied for small B, because it is inconsistent with their use of $\hbar q^2 / 2m\omega_c$ as the expansion parameter, which implies a small wave-number, large-B expansion. The expansion we have employed in the Bose case is in the first instance a small-B expansion, with full wave number and density dependence carried in the coefficients. Small wave-number expansions of the coefficients are carried out later. The expansion has been shown to be self-consistent for the various regions discussed.[15]

In Horing, Orman, and Yildiz,[9] expressions for the conductivity components are given in an integral representation, having been derived in the RPA using Green's-function techniques. In a later paper,[10] these expressions are evaluated explicitly for the high-field case (where only the lowest Landau level is occupied) in terms of incomplete gamma functions. Although the details of the Green's-function procedure were not presented, we note[9] that the cross terms were given in terms of the "longitudinal" component σ_{yy} as (using our notation)

$$\sigma_{xy} = \frac{i}{x} \frac{\partial}{\partial q^2} (q^2 \sigma_{yy})$$

$$= -\sigma_{yx} . \tag{39}$$

Applying this formula to our expression (28) for the σ_{yy} component in the Fermi plasma with $B > B_c$, we find that the result agrees with the σ_{xy} component for the Bose plasma.[15] This is precisely our result for the Fermi plasma if the spin terms are neglected. Thus we conclude that the electromagnetic effects of spin were neglected in the Green's-function treatment.[9,10] This omission is particularly serious in the latter paper,[10] where strong-field (i.e., $B > B_c$) results are presented. In the final results of that paper, in addition to the relation (39) above, a further relation connecting the "transverse" component σ_{xx} with the "longitudinal" component σ_{yy} is quoted:[10]

$$\sigma_{xx} = \frac{i\rho e^2}{\mu\omega} + \frac{1}{x^2}\left[1 + \frac{\partial}{\partial q^2} + q^2\frac{\partial^2}{\partial(q^2)^2}\right](q^2\sigma_{yy}) . \quad (40)$$

Application of this relation to our expression for σ_{yy} yields the corresponding Bose result for σ_{xx} indicating again that spin has been neglected and that Eq. (40) is incorrect in the Fermi case. When spin is correctly incorporated into the conductivity treatment, the relation (40) above is replaced with the remarkably simple result

$$\sigma_{xx}^{B>B_c} = \sigma_{yy}^{B>B_c} . \quad (41)$$

The inclusion of spin in the conductivity derivation, at the expense of a somewhat more complicated formalism, leads to significantly different conductivity components. In the $B > B_c$ case for which the tensor has been explicitly evaluated, a considerable simplification of the results for σ_{xx}, σ_{yx}, and σ_{xy} is found. This leads to a less cumbersome dispersion relation (31) than is obtained if spin is neglected.

Despite the drastic effect on the structure of the dispersion relation, we find that the inclusion of spin does not significantly affect the plasmon dispersion in the plasma layer. This is a result of the nature of the spin corrections to the conductivity tensor and the structure of the coupled dispersion relation. The σ_{xx}, σ_{yx}, and σ_{xy} components contain terms due to spin, which are of order z, while the "longitudinal" component σ_{yy} contains no spin terms. In the low wave-number regions where transverse effects are important in the dispersion relation, the parameter z is extremely small and, as a result, so also are the spin corrections. At larger wavelengths where the spin corrections to these components are significant, the dispersion relation is dominated by the longitudinal branch (involving σ_{yy}), and again the effect of spin on the dispersion relation, though readily apparent numerically,

is very small. The structure of the conductivity tensor for $B < B_c$, and the influence of the spin terms on the dispersion relation in that region, where de Haas–van Alphen oscillations occur, remain important topics for further investigation. It is clear that extensive numerical work is required to investigate the large range of field strengths and densities of interest. For this purpose the integral representation developed by Glasser,[12] which isolates the Bernstein singularities from temperature and magnetic-field dependencies, could prove useful if applied to the complete conductivity tensor displayed in Eq. (20).

As was noted in Sec. I, the formalism developed here for the inclusion of spin in the conductivity tensor, summarized by Eq. (8), should be applied in the bulk plasma as well as the plasma layer investigated here. In the three-dimensional case, plasmon modes propagating perpendicular to the applied magnetic field, with associated electric fields also perpendicular to the B field, must satisfy the dispersion relation[17,18]

$$4\pi i\omega\left[\sigma_{xx} + \frac{\sigma_{xy}^2}{\sigma_{yy}}\right] = q^2c^2 . \quad (42)$$

This dispersion relation describes the so-called "extraordinary waves," which contain both longitudinal and transverse components. Unlike the two-dimensional case, however, there is no retardation effect and consequently no reason to expect any restriction of transverse effects to small wave numbers. This reflects the fact that in the unmagnetized three-dimensional plasma, both transverse and longitudinal plasmon modes are found, in contrast to the unmagnetized two-dimensional plasma where only longitudinal modes occur. Thus the investigation of spin effects in bulk plasmas, requiring the evaluation of Eq. (8) using three-dimensional matrix elements, would be of considerable interest.

[1] High Temperature Superconductivity, edited by J. W. Lynn, Graduate Texts in Contemporary Physics (Springer-Verlag, New York, 1990), and the extensive list of references therein.

[2] F. Stern, Phys. Rev. Lett. 18, 546 (1967).

[3] T. Ando, A. B. Fowler, and F. Stern, Rev. Mod. Phys. 54, 437 (1982).

[4] K. W. Chiu and J. J. Quinn, Phys. Rev. B 9, 4724 (1974).

[5] G. Fasol, D. Richards, and K. Ploog, in Condensed Systems of Low Dimensionality, edited by J. L. Beeby et al. (Plenum, New York, 1991), p. 35.

[6] E. G. Harris, in Advances In Plasma Physics, edited by A. Simon and W. B. Thompson (Wiley, New York, 1969), Vol. 3, p. 157.

[7] N. J. Horing, Ann. Phys. (N.Y.) 31, 1 (1965).

[8] N. J. Horing and M. M. Yildiz, Ann. Phys. (N.Y.) 97, 216 (1976).

[9] N. J. Horing, M. Orman, and M. Yildiz, Phys. Lett. 48A, 7 (1974).

[10] N. J. Horing, E. Kamen, and M. Orman, Physica 105B, 115 (1981).

[11] N. J. Horing and M. Yildiz, Phys. Lett. 44A, 386 (1973).

[12] M. L. Glasser, Phys. Rev. B 28, 4387 (1983).

[13] D. C. Bardos and N. E. Frankel, Physica A 189, 282 (1992).

[14] N. S. Witte, V. Kowalenko, and K. C. Hines, Phys. Rev. D 38, 3667 (1988); J. Daicic and N. E. Frankel, Prog. Theor. Phys. 88, 1 (1992).

[15] D. C. Bardos, D. F. Hines, and N. E. Frankel, preceding paper, Phys. Rev. B 49, 4082 (1994).

[16] V. Gudmundsson, T. Toyoda, and Y. Takahashi, Phys. Lett. 100A, 91 (1984).

[17] E. A. Kaner and V. G. Skobov, Plasma Effects In Metals (Taylor & Francis, London, 1971), p. 88.

[18] D. G. Lominadze, Cyclotron Waves In Plasmas (Pergamon, Oxford, 1981), p. 13.